Systematic Design of a Heaving Buoy Wave Energy Device

Hongda Shi[1], Dong Wang[1], Jinghui Song[2], Zhe Ma[3]
1 Engineering College, Ocean University of China;
Qingdao,Shandong,China
E-mail: hd_shi@ouc.edu.cn

2 Qingdao Port International Co., Ltd
Qingdao, Shandong, China
E-mail: songjinghui1989@163.com

3. National Oceanographic Centre Qingdao.
Qingdao, Shandong, China
E-mail: mzzz-222@163.com;

Abstract

Oscillating type devices constitute a major class of offshore wave energy converters. In view of the characteristic of the wave energy in China that is low in energy density, a new heaving buoy wave energy device is designed. The paper introduces the basic components of the device, including buoys, support platform, submerged platform, anchor system and hydraulic power take-off, addresses the system design of the device and explains the working process of the converter. The physical experiment is performed in Shandong Provincial Key Laboratory of Ocean Engineering, China. The result shows that the heaving buoy wave energy device is simple, the energy acquisition system is stable and the efficiency is high.

Keywords: Wave energy; Heaving body; Systematic design; Support platform; Power take-off

1. INTRODUCTION

Wave Energy have being developed for morfe than 200 years. The first patent for wave energy converter could date back to 1799 by the Girard[1]. For the past decades, wave energy's development has being a rather hot field. Much more than1000 patents was filed.

Among all the devices that was filed, heaving buoy is an important form. It is named the 3rd generation wave energy convertor. The device contacts the wave directly so its conversion efficiency is really high. Also it is much smaller than other forms. What's more, it is adaptable to various of water depths with the help of mooring system. A device named Archimedes wave swing by Teamwork Technology BV claimed to had reach the capacity of2MW.[2] That's why this type was chosen to be the wave energy convertor of "300kW Ocean Energy Integrated Power Supply System" project in China.

According to Hulme's research, the best radius for single buoy can be calculated by $a=0.262T^2$.[3] It is tested that the buoy of best radius only response to a narrow width of frequency efficiently. However, the wave in the real sea was combined of different kind of frequency, especially in China sea. Moreover the size of the buoy with best radius is very bigger, which makes it not that economic. For these reason, the heaving buoys was invented. One of that device consist of several single buoys with smaller radius. This article focuses on the study of this form.

This device, named the heaving buoys, and it is made up of 2 parts: the upper structure and the mooring system.

1.1 The upper structure

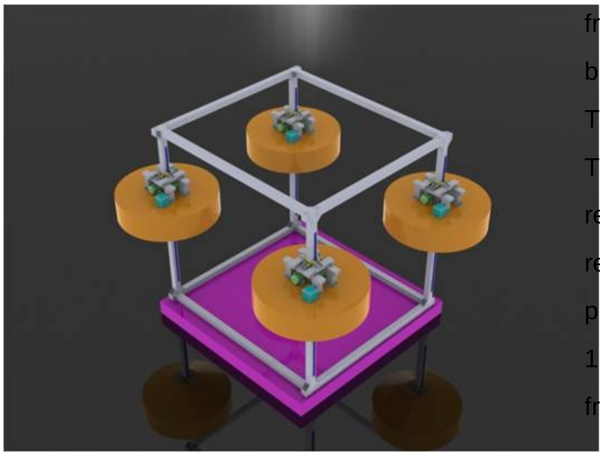

Fig. 1. the design sketch of the upper structure

The upper structure is the main part of the device. It contains of two system: electrical power generation system (EPGS) and the support system.(Fig. 1)

Electrical power generation system consists of four buoys, hydraulic rams and pistons, hydraulic piping, hydraulic motor and rectification. The buoys interaction with waves and absorb the energy contains in the waves. With this energy they push or pull the pistons and make the hydraulic oil circulate in hydraulic rams and piping. In turn, the oil impact the hydraulic motor which is connected to an electric generator. Finally, the rectification will adjust the electricity from four buoys to the same phase and make them into one. (The hydraulic system was not given in Fig.1)

The support system consists of 3 parts: the submerged part, framework and the platform. The submerged part is a floating structure and fixed to the bottom by the tentioning chain of the mooring system and by that way we can believe that the submerged one is fixed in vertical direction. It is below the water surface and provides the buoys with a reference of movement. (The violet part in Fig. 1) The framework run through the middle part of the buoys and limited it to one degree of freedom. The platform is on the top of the framework. The hydraulic piping, hydraulic ram, rectification as well as the detection and recondition equipment is installed on the platform. The platform was not given in Fig. 1,but you can image it being fixed on the top framework..

1.2 The mooring system

The mooring system of heaving buoys is shown in Fig. 2. It fixed the submerged part static to the bottom, so it makes the device adaptable to the depth range from 10-40 meters. Also it provides a resistance to the influence of tidal range. First, an anchorage foundation (or balance weight) is placed at the bottom. In reality, it is an iron cage filled with rock blocks. Then several anchor chain is used to pull the submerged part towards the anchorage foundation. The left part of Fig. 2 show one layout of the mooring system with 8 straight anchor chains.

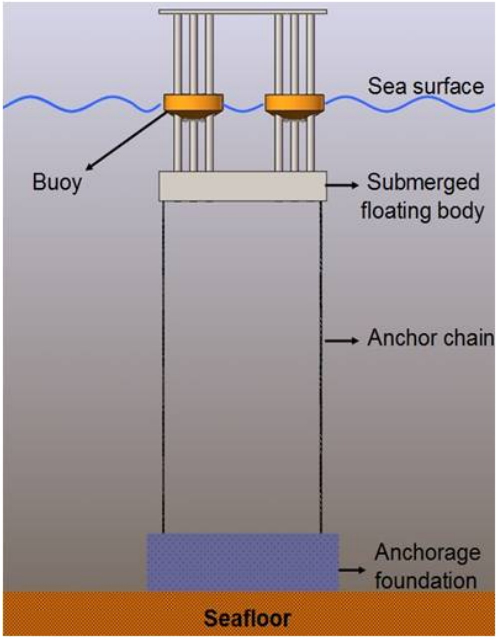

Fig. 2. the design sketch of the mooring system

2. THEORETICAL ANALYSIS

The theoretical analysis was divided into 2 steps, analysis based on Newton's 2nd law and the one based on potential function theory. In both of the analysis, the below assumption is used.

1) The fluid is incompressible, non-viscous; The movement is irrotational;

2) The waves are assumed to be small amplitude ones, which means the length of the wave outstrip the height;

3) The wave s are simple harmonic ones;

4) The water body is unlimited in horizontal orientation and equality in depth;

5) The movement of the buoy is simple harmonic ones;

6) The buoys are modulated to the best phase and amplitude condition.

2.1 Analysis based on Newton's 2nd law

A diagram calculation model is given. (Fig. 3) As can be seen, only the cylinder buoy's analysis is given as an example.

Assumes the wave surface is in line with $\zeta = \zeta(t) = ae^{i\omega t}$, the movement of the buoy is in line with $H = H(t) = Ae^{i\omega t+\phi}$. Then assume that the density, radius, height and thickness of the buoy is ρ_0, r, h, d respective.

The mass of the buoy is calculated by

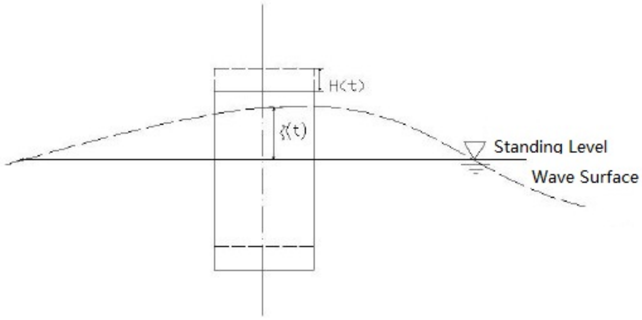

$$m = \rho_0 V_0 = 2\rho_0(\pi r^2 + \pi rh)d$$

Fig. 3. Calculation model

(1) The acceleration of it is expressed

$$a = \frac{d^2H}{dt^2}$$

(2) There are three forces act on the buoy, the gravitational one, the resistant one, and the buoyance.

In theoretical analysis, the resistant force is only rised by the hydraulic system. So it can be expressed by:

$$F_f = \frac{9550p}{nr_t}, \text{ where } n = \frac{30}{\pi}\frac{v}{r_t};$$

The gravitational one and the buoyance is summed up as the net buoyance, which can be expressed by:

$$\Delta F_b = \rho_w g S[\zeta(t) - H(t)];$$

So the joint force can be expressed by:

$$F = \Delta F_b - F_f = \rho_w g S[\zeta(t) - H(t)] - \frac{30}{\pi}\frac{v}{r_t};$$

(3)Bring all the factors numbered 1, 2, 3 into

Newton's 2nd law F=ma, we will get this equation.

$$-\rho VA\omega^2 e^{i(\omega t+\phi)} = \rho_w gS\left[ae^{iwt} - Ae^{i(\omega t+\phi)}\right] - \frac{9550\pi}{30i\omega e^{i(\omega t+}}$$

(4)According to the Euler equation:

$$e^{2i\omega t} = \cos(2\omega t) + i\sin(2\omega t);$$

$$e^{2it} = \cos(2t) + i\sin(2t);$$

$$e^{i\phi} = \cos(\phi) + i\sin(\phi);$$

Equation 4 can be calculated and the amplitude of the movement of the buoy can be given as below:

$$A = \frac{-3\omega\rho_w gSa\sin(2\omega t+\phi)}{6\omega(\rho V\omega^2-\rho_w gS)\sin(2\omega t+\phi)} \pm \frac{\sqrt{[-3\omega\rho_w gSa\sin(2\omega t+\phi)]^2}}{6\omega(\rho V\omega^2-\rho_w gS)\sin(2\omega t+\phi)} - \frac{\sqrt{12\omega(\rho Vw^2-\rho_w gS)\sin(2\omega t+\phi955P\pi)}}{6\omega(\rho V\omega^2-\rho_w gS)\sin(2\omega t+\phi)}$$

Based on these result, we analysis the motion response of the buoy with different shape.

In this case, we set the figure as below: The density of the material used for the buoy is $7850 kg/m^3$; The thickness of the buoy 0.02m; The height of the buoy is 1m; The gravity is 9.8 N/kg; The power of the generator is 1kW; The density of the water is $1025 kg/m^3$.

The models analysised is buoys of 3 kind of shape: the cylinder one, the cylinder with cone bottom, and the one with sphere bottom.

Fig. 4 show the displacement relative to time of 3 shapes of buoy. The one on the left show the movement of the cylinder buoy. The one in the middle shows the movement of the cylinder with cone bottom. The one on the right shows the movement of the cylinder with sphere bottom. It show the cylinder one and the cylinder with sphere bottom ones moves more stable. The cylinder with cone bottom ones moves move shape but in disorder.

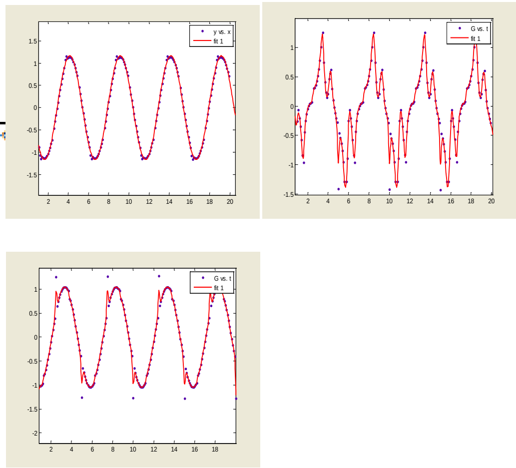

Fig. 4. Simulated displacement figures

2.2 Analysis based on potential function theory

In this stage of analysis, four steps should be dong.

1) Give the governing equation, boundary condition and solve the problem to get the potential equation.

2) Work out the exciting force and other hydrodynamic coefficient.

3) Solve the kinetic equation.

4) Get the power absorbed by the buoy and the amplitude of the buoy.

In the first step, based on the assumption above, the fluid body conforms to Laplace equation or equation of continuity. According to the Bernoulli equation, the fluid pressure can be expressed by this equation: $\frac{p}{\rho} = -\left(gz + \frac{\partial\phi}{\partial t} + \frac{1}{2}|\nabla\Phi|^2\right) + c(t)$.[4] The boundary condition is divided to surface condition ($\frac{\partial\Phi}{\partial n} = \bar{u}_n$ or 0) and free surface condition. ($\frac{\partial^2\Phi}{\partial t^2} + g\frac{\partial\Phi}{\partial t} = 0$). we divide the velocity potential into three parts: the incident one, the diffracted one and the radiated one. $\Phi(x,y,z,t) = \Phi^I(x,y,z,t) + \Phi^D(x,y,z,t) + \Phi^R(x,y,z,t)$. Arrange the governing equation and boundary condition for each components of the velocity potential.

In the second step, the exciting force consists of incident force and diffracted force.

$F_{ej} = F_{kj} + F_{dj} = \mathrm{Re}\{(\ddot{F}_{kj} + \ddot{F}_{dj})e^{-i\omega t}\}$, in which $\ddot{F}_{kj} = \rho i\omega \iint \Phi^{I} n_j dS$, $\ddot{F}_{dj} = \rho i\omega \iint \Phi^{D} n_j dS$.

Those equations are beyond the calculating ability, so numerical computation method is adopted in solving this problem. Due to the useful data are all in the boundary, the BEM is used in this project.[5]

In the third step, the kinetic equation is solved: $ma + \rho gSx = F_k + F_d + F_r + F_{PTC}$.

The result shows the influence of the mass, size and shape on the efficiency of buoys each.

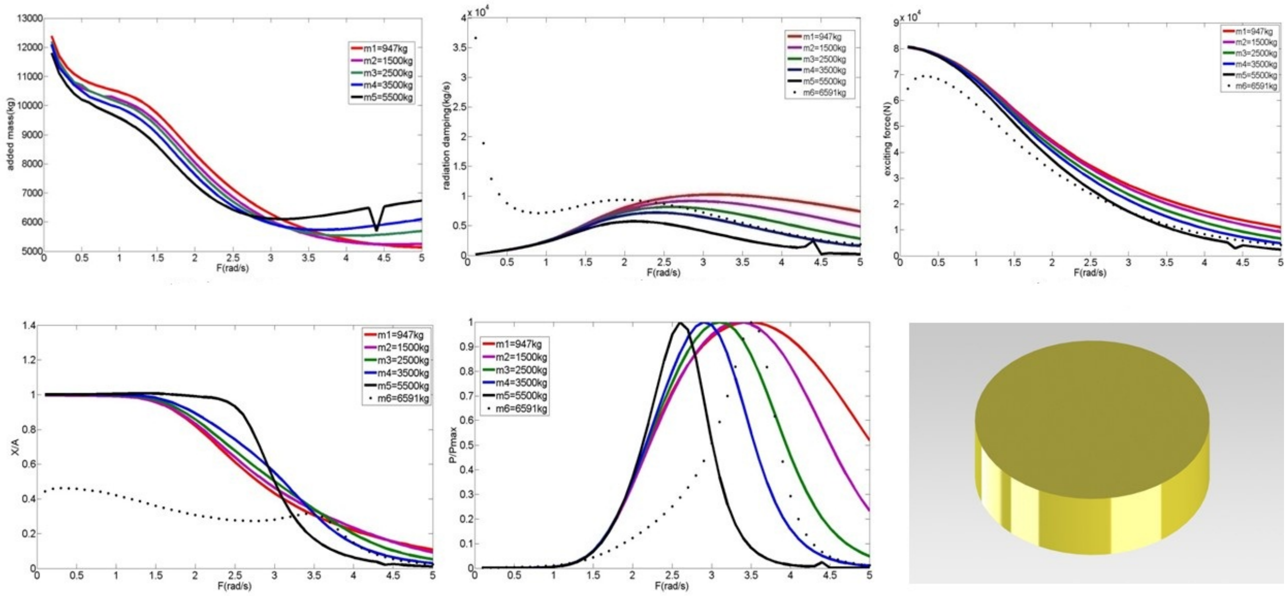

Fig. 5. Result of cylinder on different mass

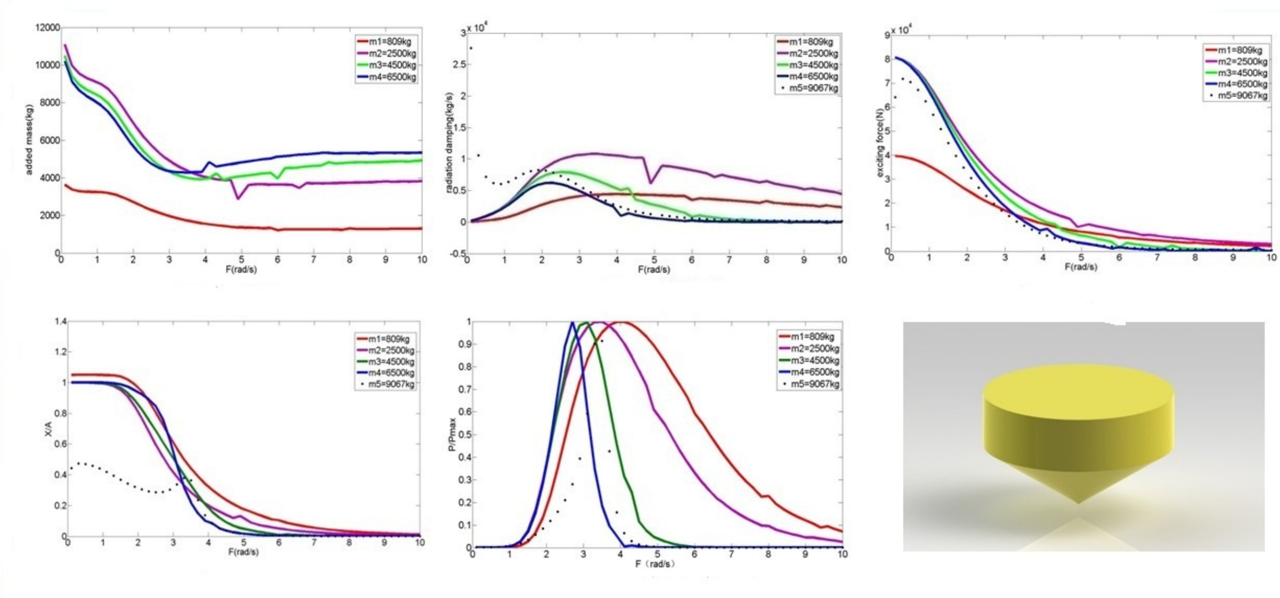

Fig. 6. Result of cylinder with cone bottom on different mass

Fig. 5 and Fig. 6 show the result of two model on different mass. The result include added mass, rotational damping, exciting force, X/A and PTO efficiency. There are also data on different radius, height, and cone angle, they are not given due to the space limit.

2.3 Analysis of the mooring system

When the device is working, the PTO of the Hydraulic cylinder will give force to the device. Then it will change the force of the anchor chains. When the buoy moving up, the PTO will give the device upward force, and vice versa. The force of the PTO cannot be measured directly, then we need to find the equivalent action form of it to analyze the influence of PTO to the mooring system.

Bernoulli's equation:

$$\frac{p}{\rho g}+\frac{v^2}{2g}+Z_1=\frac{p'}{\rho g}+\frac{v'^2}{2g}+Z_2 \tag{5}$$

Mass conservation: $v\cdot A=v'\cdot A'\rightarrow v'\frac{v\cdot A}{A'}$

(6)

The overall efficiency of hydraulic pump η_t is the ratio of actual output power to input power, while it is equal to the product of volumetric efficiency η_m and mechanical efficiency η_v, in which η_m=0.9×0.95; $\eta_v=0.98$. The equation can be write as $\eta_t=\frac{p'Q'}{pQ}$, according to the flow conservation: Q'=Q, so a proper relationship can be defined as $p'=\eta_t p=\eta_m\eta_v p$ (7)

Eq. 5,6,7 can be deduced as

$$\frac{p}{\rho g}+\frac{v^2}{2g}+\frac{\eta_m\eta_v P}{\rho g}+\frac{A^2}{2g\cdot A'^2}v^2+\Delta Z \tag{8}$$

After neglect ΔZ, and make $\alpha=\frac{\rho(A^2-A'^2)}{2(1-\eta_m\eta_v)A'^2}$,

then $F_{PTO}=\alpha AV^2$ (9)

Where p is the pressure of the piston, v is the velocity of movement of the piston, also it is the velocity of movement of the buoy, v' is the pipe flow velocity at the entrance of hydraulic motor, ρ is the density of the hydraulic oil, A is the hydraulic cylinder piston area, A' is the pipe inner area at the entrance of hydraulic motor.

According to the final equation, we can get the force data from the velocity of movement of the buoy.

3. NUMERICAL SIMULATION

3.1 Numerical simulation theory

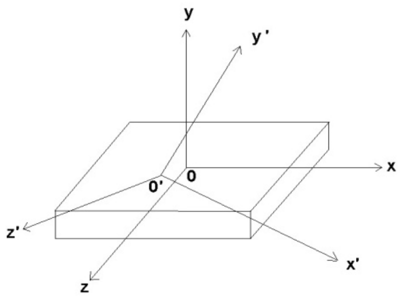

Fig.7. The coordinate systems

To express and analyze the movement of the floating body conveniently, two coordinate systems are adopted (see in Fig. 4): reference coordinate system 0'-x'y'z' and the moving coordinate system 0-xyz[6].

In the moving coordinate system, the time domain equations of motion for floating mooring system [7] :

$$(M+m)\ddot{x}(t)+\int_{-\infty}^{t}K(t-\tau)\dot{x}(t)d\tau+Cx(t)=F_w(t)+F_{wind}+F_e+F_{sn}(t)+F_m(t) \tag{10}$$

Where M and m were the generalized and additional mass matrix, K(t-τ)was the delay function matrix of the system, C was the static water's restoring force coefficient matrix of the floating body, Fw(t), Fwind, Fc,, Fsn(t), Fm (t) were the first-order wave force, wind force, the force of tide, the second-order wave force, anchor chain's tensile force. According to Cummins's [8] theory about the convolution relationship between time domain and frequency domain wave forces, the first-order wave force can be calculated. The simulation of second-order wave force use Newman [9] approximation method. According to indirect time-domain method, it can use the Green function of frequency domain method to calculate the floating body additional mass, damping, and wave forces, transform frequency domain hydrodynamic coefficients into the time-domain hydrodynamic coefficients by Fast Fourier Transform (FFT) [10].

The software of numerical simulation is Flow-3D. This software is based on fully discrete Navier - Stokes equations, using the control volume method which scalar variables in a grid body heart and vector variables on the grid surface's heart, then it would be helpful to the stability of numerical calculation and easy to solve. It use FAVOR, FDM and TruVOF respectively to describe complex geometry and accurate free surface simulation. Then complete the force analysis of the object in the fluid-structure interaction phenomenon.

(1) Base on Reynolds averaged N-S equation and VOFmodel, a 3D numerical wave tank was established. Premising on satisfying the numerical simulation accuracy, the grid is divided into three parts. On both sides we set grid with large size and refined it in the middle part. Fig. 8 show the mesh used in the simulation of mooring system. On both sides of the grid size is 0.4, the middle section of grid refinement to 0.2. The wave tank is 12 m wide, 20m deep and 110m length. The device is placed in the middle part with length of 38m. Incident wave is linear wave with 2.0m height and 4.0s period.

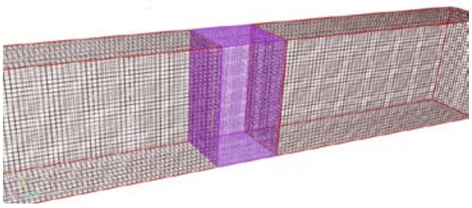

Fig. 8. The division of the grid.

(2) The boundary setting as follows: the bottom is wall, the top is atmospheric pressure, the flow boundary is outflow (allow fluid to enter at outflow boundary) and using Porous media to accomplish wave absorbing [11], According to the research achievements of Karim, the porosity of porous media set to 0.8[12].

Fig.9 shows the boundary setting.

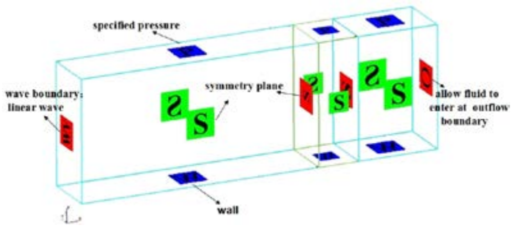

Fig.9. boundary setting

(3) Use the STL file importing command to import the model, set the related parameters in the drop-down list to complete the location then the model importing is completed. For the simulation of mooring system, the chains should be added and the modality be chosen as elastic rope, spring coefficient set as 1e+06.

Fig. 10 show the model for mooring system and Fig.11 show the simulation for single buoy.

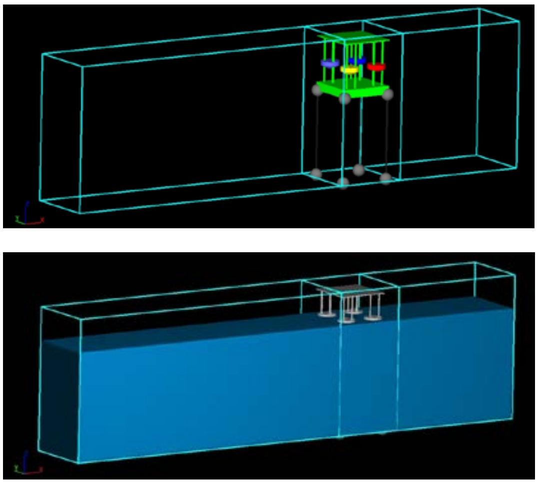

Fig.10. Model figure

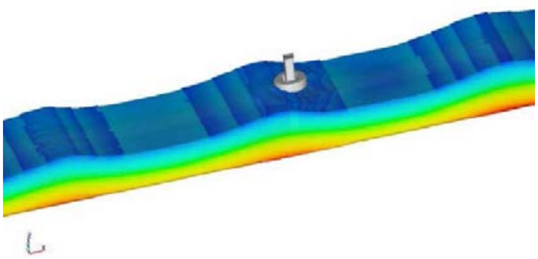

Fig. 11. Simulation for single buoy.

3.2 Numerical of the upper structure

In the simulation of the upper structure, the simulation of single buoy's kinetic characteristic is the main part. In these simulations, two type of tank was used as is shown in Table 1.

Table 1. Tank used in simulation

	Tank1	Tank2
Length(m)	60	400
Width(m)	3	16
Height(m)	1.5	21
Depth(m)	0.8	16

First of all, to test the result of the theoretical analysis, a series of simulation was carried out. In these simulations, the buoy was not placed in the tank. We captured the waveform 5 and 21 minutes after the wave coming in. The process of the wave propagation can be clear seen in Fig. 12.

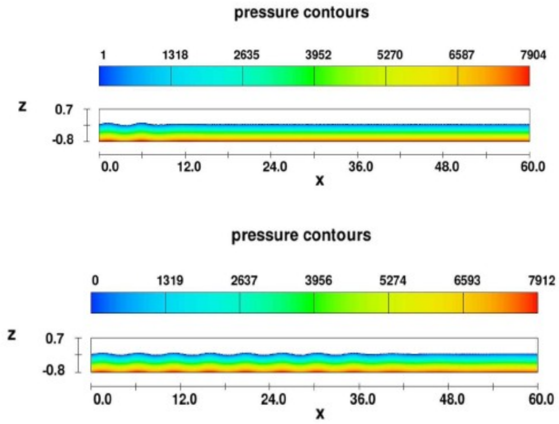

Fig. 12. The wave propagation

Then 4 points with the distant of 5m, 10m, 15m 20m to the beginning of tank I were chosen. The wave curve relative to time is captured. These figures show after several period the movement of the water particle is stable. And the height, the period and the length match well with data by theoretical analysis. Two of the figures is given below.

On the Second stage, we placed a single buoy into the middle of the tank. (both tank) Simulate the effect of the power take-off system with a one-way spring. The figures of the buoy are shown in Table 2. The model based on the gravity similarity.

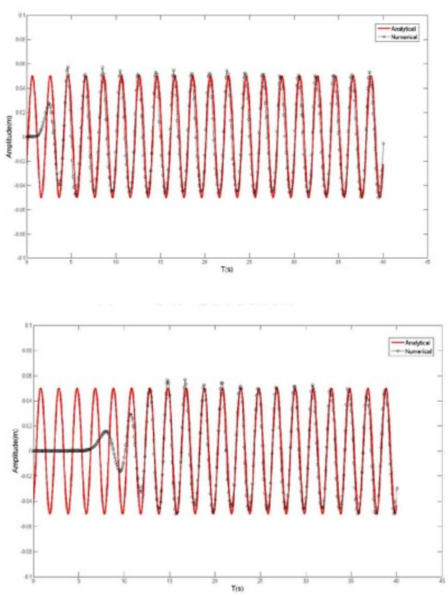

Fig. 13. Wave curve relative to time at 5m (left) and 20m (right)

Table 2. Figures of buoys used in the simulation.

	Cylinder		Cylinder with cone bottom	
	model	prototype	model	prototype
Diameter(m)	0.8	3.2	0.8	3.2
Height(m)	0.2	0.8	0.4309	1.7328
Cone angle(°)	0	0	120	120
Weight(kg)	37	2368	37	2368

In order to reach 10kW of output, the force act on the piston of the hydraulic system is $F_d = 10^4 \cdot \Delta p_d \cdot A$ =11674.5N. Assume the stroke of the hydraulic ram is 2 meters and the elastic strength is calculated to be 23349N/m. The results show below. The blue curve shows the movement of the water surface and the green one show the movement of the buoy. It can be told from Fig. 14 that the movement of the buoy is not sinusoid. The ascent stage is faster than the declining stage. The introduction of the power take-off system has increase the period of the buoy for around a quarter of the wave period.

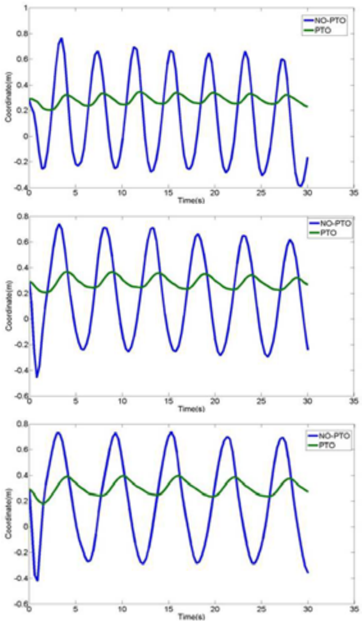

Fig. 14. Movement of the buoy and water surface with wave period of 4, 5 and 6 second

3.3 Numerical of the mooring system

The working condition of the device is as follows. The depth of the water is 20.0 m. Based on the axial symmetry of the device, it is placed at the center. 0x axis is assumed the incident direction. Under normal circumstances: wind speed is 4.0 m/s and the surface velocity is 2.0 m/s, the significant height of wave is 0.6 m; period is 4.0 s. Under the extreme conditions: the surface velocity is 25.0m/s; the height of wave is2.0 m; the period is 4.0 s. The extreme conditions is the main point of calculate.

Table 3 shows the device's size and parameters in the simulation.

Table 3. Device's size and parameters

Item	Non-working state	Working state
Submerged floating device size S_s /m	8.09X8.09X1.0	
Height of stake H_s /m,	8.0	
Diamater of floater D_f /m	3.2	
Length of anchor chain L_a /m	16.0 (Straight)	
Dead weight of device W_d /t	93.9	
Submerged depth of Submerged floating device D_s /m	4.0	5.4

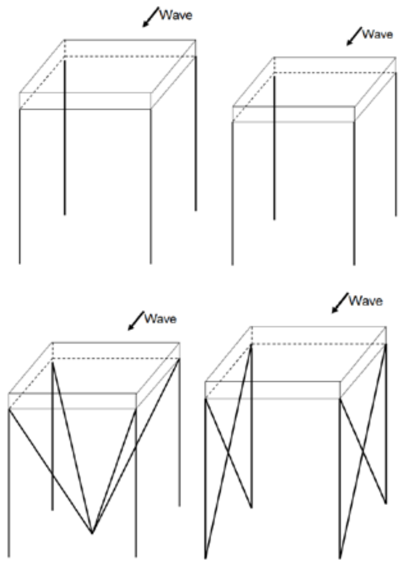

Fig. 15. The anchoring scheme

Based on previous study, four schemes need to be studied to find the best plan.

Using the above method and the data in table 3 to calculate the force of mooring system with 4 anchors, then we can analyze the influence of PTO to mooring system. Meanwhile, we will analyze the 4 anchoring schemes in Fig.15 by calculating the longitudinal motion amplitude of each scheme.

Eq(9) shows the relationship between F_{PTO} and v, then we obtain the data about F_{PTO} by ascertaining v.

Use a software Flow-3D to give a numerical simulation of the case study. Finally we can obtain the following data. Fig.16 shows the difference about the force of the mooring system (4 anchors) between load(PTO) and no-load(without PTO)

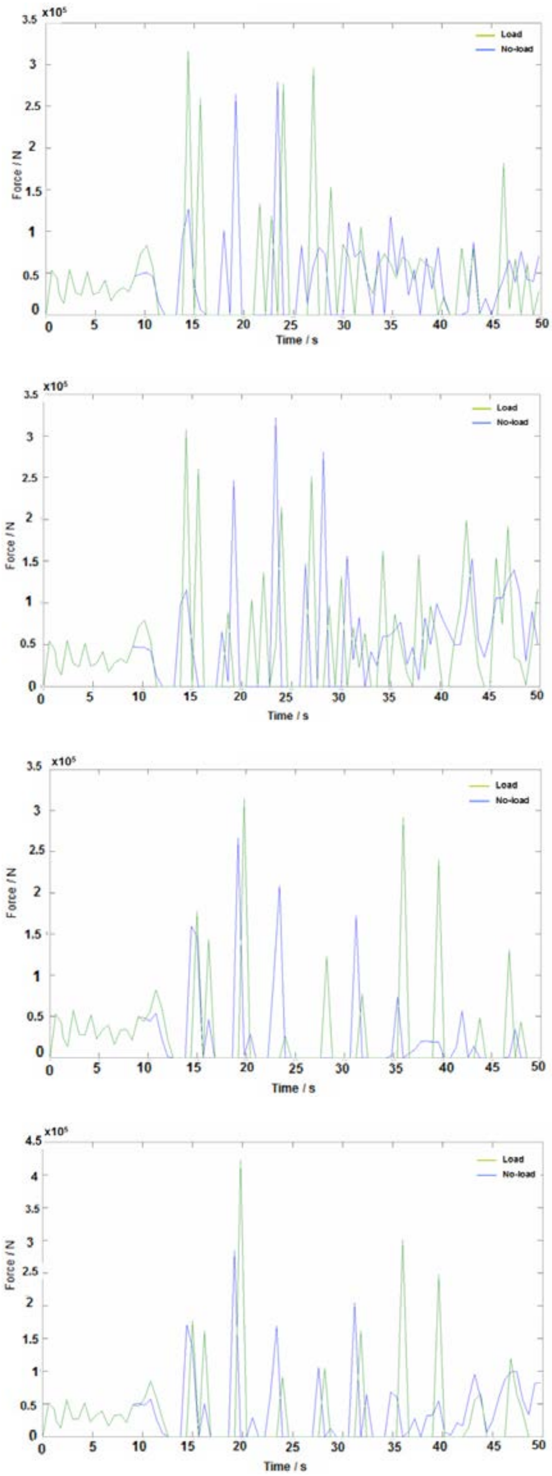

Fig. 16. The difference about the force of the mooring system between load(PTO) and no-load(without PTO)

Because of the affect of PTO, the maximum force of the mooring system is increased and the minimum is decreased. So we need to choose higher levels of anchor chains.

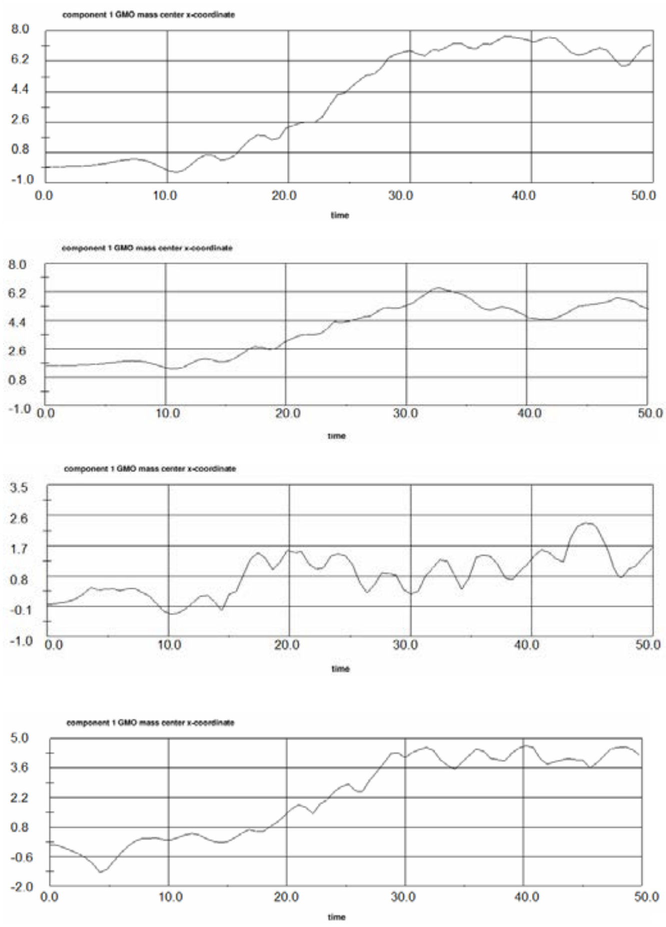

Fig. 17. The longitudinal motion amplitude of the plan I, II, III, IV.

Contrast the four figures above, the mooring systems of plan I own the worst stability because of its minimum rigidity of system. Plan II is better than plan I, but it's still not enough. Plan III have the least longitudinal motion amplitude, then it have the best stability of all. Plan IV is the second choice.

4. PHYSICAL MODEL EXPERIMENT

Till now, 4 main experiments have been carried out. The first one conducted at December 2011 is called the performance test. Its main purpose is to test the influence of freeboard and displacement. The second one began at December 2012 is named the single buoy experiment. These experiment are to study the performance of the buoy while there is power take-off. Based on the single buoy experiment, a sea-trial on single buoy was carried out on August 2013. After a series of difficulty, finally it succeeds. At the same time, the experiment on the mooring system was carried out, too. It is a qualitative experiment to see the stability of all the plans.

Presently, two experiment is conducted. Experiment on combine has replace the gear and spline system to hydraulic system, and the model consist of 4 buoys as the prototype. Sea-trial on a prototype capable of 10kW began at January 2014.

In this article, only the single buoy experiment and the mooring system experiment are introduced..

3.1 Single buoy experiment

The two models used in these experiments are shown in Fig. 18. Balancing weight is used to change the inertance of the buoy. The working condition shows in table 4.

Table 4. Working condition.

No.	Factor	Model	Weight (kg)	Height (m)	Period (s)
1	Wave Height	I	37	0.0625	2.0
				0.125	2.0
				0.25	2.0
		II	37	0.0625	2.0
				0.125	2.0
				0.25	2.0
2	Period	I	77	0.25	2.0
				0.25	2.5
				0.25	3.0
No.	Factor	Model	Weight (kg)	Height (m)	Period (s)
2	Period	II	77	0.25	2.0
				0.25	2.5
				0.25	3.0
3	Shape	I	37	0.25	2.0
		II	37	0.25	2.0

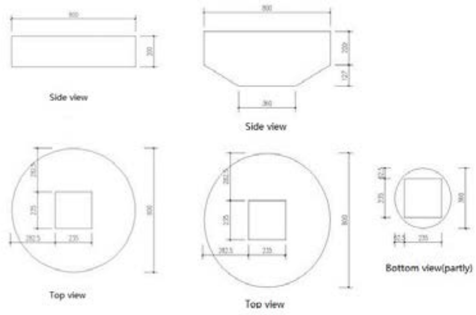

Fig. 18. Models

The three figures below show the result from the experiment. Fig. 19 shows the result from model I. The left 2 pictures show the study of height. They correspond 1-I in table 4 and show the velocity of the buoys increase with the height of the wave. The right 2 pictures show the study of period. They correspond 1-II in table 4 and show there is a peak around resonance period. Fig. 20 shows the result from model II. The trait of movement is same with model I but it show move obvious effect of resonance period. Fig. 21 shows the trait of movement when 50W generator, 0-35Ω resistance and 1:18 accelerator is introduced to Model II. As the increasing of the height of wave, the velocity of the buoy increases, too. (first picture) The output power increases even obviously. (second picture) As for the period, the velocity of the buoy has a peak around the resonance, too. But the output power drops with the increase of the wave period. (3rd and 4th picture)

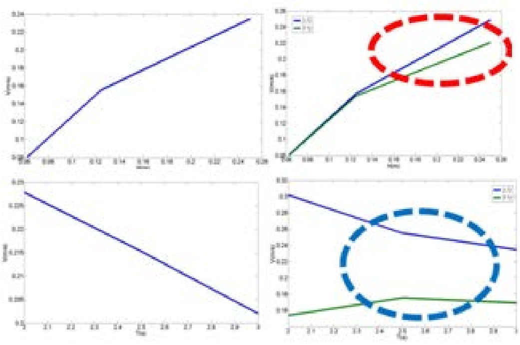

Fig. 19. Result on model I

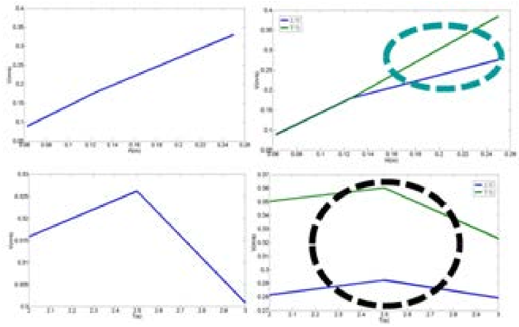

Fig. 20. Result on model II

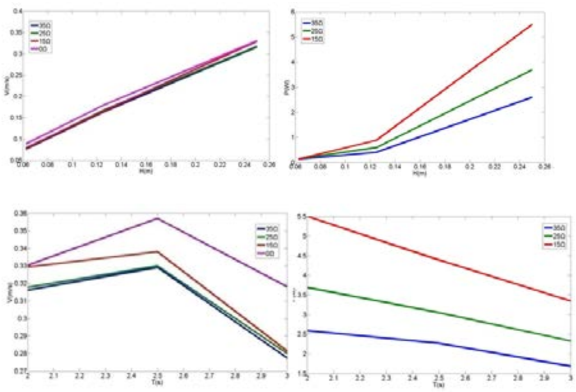

Fig. 21. Result on model II with electrical resistance

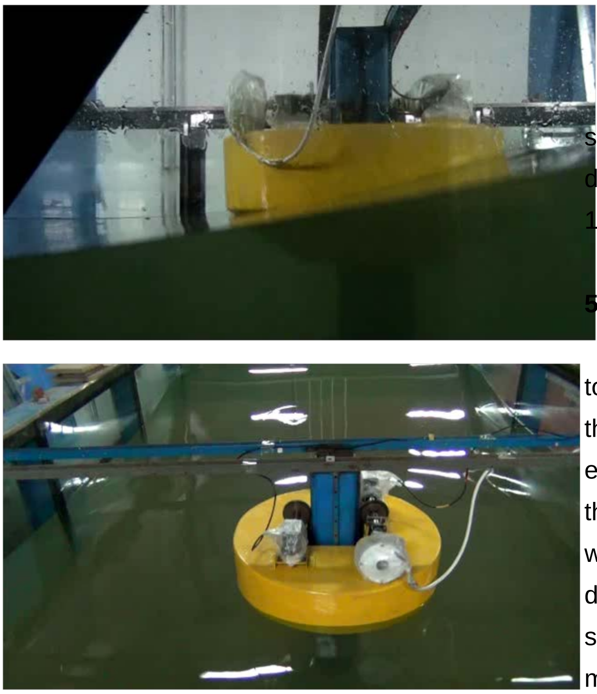

Fig. 22. Model II with 25Ω resistance is conducting

3.2 Mooring system experiment

In the mooring system experiment, the scale of model adopted was 1:10. The buoy diameter is 320mm. The pillar height is 1000mm and the gap between buoys is 800mm. The submerge structure is 1000×1000×150. There were four schemes to be tested in these experiments as below. The one with 4 straight anchor chain is not stable enough. The other three schemes in the experiment: the straight one, the inclined one and the hybrid one as is shown below

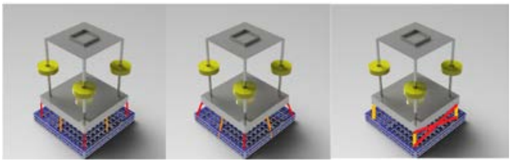

Fig. 23. Mooring system schemes

The working condition shows as below.

Table 5. Working condition for mooring system

Water level	Wave factor	No. of anchor	Anchoring form	Balance weight
0.6m	H=0.1m T=2s	4	Straight	None
1.0m	H=0.2m T=2s	8	Straight, inclined and hybrid	20kg

The result shows the hybrid mooring system perform the best with the lateral deviation of the upper structure no more than 10 centimeters.

5. CONCLUSION

1. The performance of the buoy has nothing to do with the height of it. On the other hand, the diameter and the cone angle influence the efficiency and moving amplitude evidently and the relationship is non-linear. While the weight increases, the resonance frequency decrease and energy absorbing domain shrinks. So it is important to determine the mass of buoys according to the condition of working environment.

2. The buoys shaped cylinder with cone bottom performed better than the cylinder ones. And the best cone angle is around 120°.

3. The peak of the output of power doesn't appear in parallel with the resonance period. So the resonance is not the sufficient condition of the highest efficiency.

4. When power take-off (PTO) system is introduced into the device, the movement of the buoy is not a sinusoid one. It moves faster upward than downward. And the period of the buoy becomes bigger than the wave period. In this experiment, the period of the buoy increased around a quarter.

5. PTO has a big influence on the force of the mooring system. When the buoy goes up, the PTO give upward force to the device and the maximum force of the mooring system is increased. When the buoy goes down, the PTO give downward force to the device and the maximum force of the mooring system is increased at some times.

6. The stability of the system depend on the rigidity of it, then the mooring system with large rigidity is the key to ensure the stability of the whole device.

REFERENCE

[1] Antonio F. and O. Falcao. 2010. Wave energy utilization: A review of the technologies. Renewable and Sustainable Energy Reviews 14:899-918.

[2] Prado M. 2008. Archimedes wave swing(AWS). In: Cruz J. edg. Ocean wave energy 90(3):90-93.

[3] Hulme H. 1982. The wave forces acting on a floating hemisphere undergoing forced periodic oscillations. Journal of Fluid Mechanics 121: 43-63.

[4] Xing Ji and Yuelong Zang. 1997. BEM development and general program. Shanghai: Tongji University Press.

[5] Benzhao Zhang and Jianan Yin. 2003. Fluid mechanics numerical method. Beijing: China Machine Press.

[6] Yue Xiao and Yanying Wang. 2004. Time-domain's calculation and analysis of three-dimensional mooring system. Dalian: Dalian Engineering University Press.

[7] Bingfu Zhang and Kun Qian. 2010. Simulation of response of moored floating body motion in shallow water. Dalian: Dalian Engineering university.

[8] Cummins. W. E. 1962. The impulse response function and ships motions: Schiffstechnic 9: 101-109.

[9] Faltinsen. O. M. 2008. Sea loads on ships and offshore structures. Shanghai: Shanghai Jiao Tong University Press.

[10] Xuejun Hu. 2007. The analysis of anchor's dynamics. Wuhan: Huazhong Science and Technology University Press.

[11] Ting Zhang. 2009. Three dimensional numerical simulation of waves and its application. Tianjin: University of Tianjin Press.

[12] Karim M. F. and Tanimoto K. 2004. Hieu P. D. Simulation of wave transformation in vertical permeable structure. International society of offshore and polar engineers. 14: 89-97.